JOURNAL OF MODERN OPTICS, 1993, VOL. 40, NO. 10, 2039–2052

Spatial light modulator used for the Fourier transformation of video images

MARTIN SCHÖNLEBER and HANS-J. TIZIANI
Institute of Applied Optics, University of Stuttgart, D-70569 Stuttgart, Germany

(*Received 18 December 1992: revision received 10 April 1993*)

Abstract. Coherent-optical Fourier transformation of video images can be very powerful; a set-up will be described. The modulation of the coherent beam occurs in a spatial light modulator where the liquid crystal display image of the object is projected onto an optically addressed spatial light modulator that uses bismuth silicium oxide for photoconduction and a twisted nematic liquid crystal as a birefringent layer. Edge enhancing of the image can occur; in addition, it appears that the Fourier spectrum of an edge is asymmetric due to local phase variations. The set-up was applied to recognize objects at different positions. A charge-coupled device matrix camera detects the Fourier plane, in the personal computer the pixels are summed up to ring-wedge-segments and processed for pattern recognition.

1. Introduction

Different photorefractive materials [1] such as bismuth silicium oxide $Bi_{12}SiO_{20}$ (BSO), bismuth germanium oxide $Bi_{12}GeO_{20}$ (BGO), bismuth titane oxide $Bi_{12}TiO_{20}$ (BTO), and barium titanate $BaTiO_3$ can be used as storage material in holography [2] and speckle techniques [3]. In this report however, BSO is applied as a transparent photoconductor layer in an optically addressed spatial light modulator (SLM) based on liquid crystals (LCs) [4]. This device was kindly provided to our institute by Thomson-CSF [5]. Its optical properties will be described in section 2.

Direct coherent-optical Fourier transformation of non-transparent, technical objects is difficult. Coherent illumination of the object's rough surface leads to the speckles, therefore the Fourier transform of the object is embedded in speckle noise. To avoid this problem spatial light modulators were applied as incoherent to coherent converters. An overview was given by Efron [6]. With a combination of a video camera and liquid crystal television (LCTV) device Casasent and colleagues [7–9] constructed a commercially available real-time (15 objects s^{-1}) Fourier transform inspection system.

In our set-up—as will be described in section 3—the LCTV image is projected onto an optically adressed SLM. The processing of the Fourier plane data occurs in a personal computer (section 4), the recognition speed is 2 Hz. We carried out some experiments on the Fourier transform of knife edges and investigated the pattern recognition performance (section 5). Some applications as detection of edges, velocity, position and results for pattern recognition will be given in section 6. In section 7 the characteristics of the set-up are summarized.

0950–0340/93 $10·00

2. The SLM unit as incoherent-to-coherent converter

In the SLM unit the video image of the object scene is first binarized and transferred to a transmittive liquid crystal display (LCD) that is illuminated homogeneously by a white light source (miniature cold cathode fluorescent lamp 8·5 V/200 mA by Matsushita). The black and white pattern produced by the LCD (290×390 pixels, area $35 \times 47\,mm^2$, contrast 1 : 100) is imaged into the optically addressed BSO/LC-SLM with a magnification of $\beta' = -0{\cdot}39$.

The BSO/LC-SLM has a layered structure. The photoconductive BSO and the birefringent twisted nematic liquid crystalline material (thickness 200 μm respectively 3 μm) are sandwiched between two electrode layers of transparent indium tin oxide (ITO). To switch the optical axis of the liquid crystal an electric field is needed. So a sinusoidal voltage ($0 \ldots 20\,V_{pp}$, $20 \ldots 100$ Hz) is applied to the ITO layers. However: in dark areas the thick photoconductor layer acts like an insulator and most of the driving voltage drops there, hence the electrical field in the LC is too small to switch. When the photoconductor is exposed to light from the LCD the full voltage drops in the LC layer and its optical axis gets turned. With polarizers before and after the SLM amplitude modulation can be achieved. The resolution of the device is 12·5 lines mm^{-1}, the maximum contrast ratio 1 : 100, and the response time 75 ms[5].

2.1. *Transmission of the BSO/LC-SLM*

In the zero voltage state of the BSO/LC-SLM the LC molecules are orientated parallel to the surface and make a successive turn of 90° between the surfaces. Light polarized parallel (mode 1) as well as perpendicular (mode 2) to the molecules at the incidence surface turns with this screw of the liquid crystal's optical axis. Because of this 'wave guiding' phenomenon one gets almost complete light extinction with parallel polarizers when its orientation is parallel to one of these wave guiding modes. Mixed mode light emerged elliptically polarized because of the run time difference of the modes.

Above a threshold voltage of 6 V the LC bulk orientation turns now pointing into the surface. As a result of the reduced waveguiding the extinction orientation of the analyser turns right-handwise (thumb pointing into the beam direction) from 5° to 30° (at 12 V), then turns back left-handwise (again 5° at 15 V, −30° at 20 V). In the 15 V driving condition of the SLM-unit bright–dark edges are enhanced (figure 4) due to the reduced effective voltage in the intermediate region.

To study the phase modulations of the BSO/LC-SLM interference of its beam with a plane reference was observed. In mode 1 the phase of the wave passing through the bright region was shifted by almost 2π when increasing the voltage from 6 to 13 V. Mode 2 did not suffer any phase-shift because its polarization remains perpendicular to the optical axis when the molecules reorientate in the electrical field.

3. The Fourier transform processor

An experimental set-up is shown schematically in figure 1. A field of $80 \times 80\,mm^2$ of the object scene was recorded by a video camera, the object distance for the camera was 500 mm. The video image was transferred to the BSO/LC-SLM as described in section 2. As a coherent light source for the read-out beam a 5 mW single mode He–Ne laser at the wavelength 632·8 nm was used. The beam passes a variable beam-splitter (VBS), a pinhole, a collimating lens, the first polarizer, the BSO/LC-SLM, the second polarizer and falls on a hologram (glass plate with dichromated gelatin).

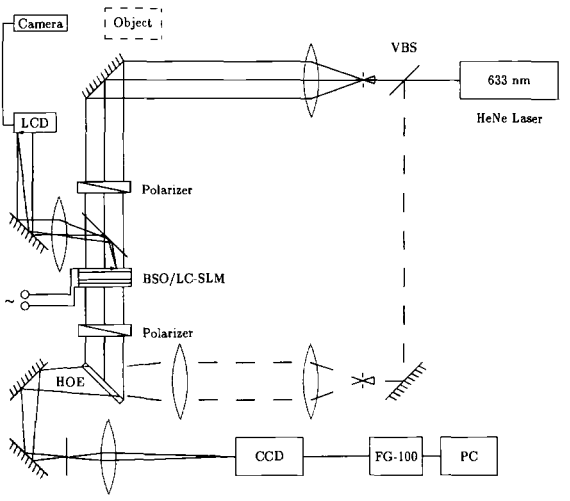

Figure 1. The coherent optical Fourier processor. Devices VBS variable beam-splitter, LCD liquid crystal display, BSO/LC-SLM optically addressed spatial light modulator, HOE holographic optical element, CCD charge coupled device, FG-100 video frame grabber, PC personal computer.

This hologram has two functions. First, it replaces a Fourier transforms lens, secondly, it eliminates phase distortions due to the BSO/LC-SLM, thus the quality of the wavefront in the Fourier plane is improved. The hologram was recorded by superimposing the read-out beam with a converging beam (the dashed path in figure 1; VBS, mirror, pinhole, collimating lens, beam converging lens ($f=240$ mm)). This path was blocked off after recording.

The diffracted part of the read-out was deflected at two mirrors. Its Fourier plane was magnified by a microscope objective and detected by a CCD video camera (Pulnix) with 512×512 pixels. An FG-100 video frame grabber digitized the frame data for further processing in an ACER 16 M Hz-386-PC. To avoid a flickering image (resulting from oscillations of LC orientation) the SLM driving voltage was synchronized to the video frequency.

4. Selection pattern attributes in the Fourier plane

A 128×128 pixels area of the Fourier plane has been segmented into wedges and concentric rings. At each 'snap' of the scene grabber the pixel intensities in the segments i are summed up. Usually we worked with ten rings and 20 wedges and used these 200 segment intensities $I(i)$ as primary pattern attributes.

In the learning phase for each reference object j a snap series was taken and the minimum and maximum intensities $I_j^{min}(i)$ and $I_j^{max}(i)$ of each segment were stored.

To each new reference the 16 'most selective' segments $i=\text{bestseg}(k,j)$ were extracted out of the 200. The principle therefore looks very simple:

Find to each old (that means already learned) reference j *at least one segment* i, *where the intensity gap*

$$I_j^{\min}(i) - I_{\text{new}}^{\max}(i) \text{ resp. } -[I_j^{\max}(i) - I_{\text{new}}^{\min}(i)]$$

to the new reference is maximal.

So, when a new reference has to be learned its most selective segments are listed and the lists of references already learned are modified taking into account the new reference.

For better understanding an example will be given: five references might have been already learned. The segment list of the first reference R_1 has 16 elements and starts with the segments where R_1 has the maximal intensity gap to the other references 2,3,4,5. How will the other 12 positions be occupied? The four 'most selective' segments of R_1 to R_2 are on the positions 1, 5, 9, 13 of the segment list, those of R_1 to R_3 on positions 2, 6, 10, 14, and so on. When a sixth reference is learned, its 'most selective' segments to each reference are inserted between the old positions 4/5, 8/9, 12/13 of each segment list. The last three of the old lists are dropped.

This procedure works safely when the number of references does not exceed the number of 'most selective' segments, 16.

The pattern recognition occurs by comparing the quadratic deviations

$$\sigma_j = \sum_{k=1}^{16} \{I_{\text{test}}[\text{bestseg}(k,j)] - \bar{I}_j[\text{bestseg}(k,j)]\}^2 \tag{1}$$

of the test object. $\bar{I}$ stands for $(I^{\max} - I^{\min})/2$.

5. Experiments

As was mentioned before, for the analysis of the spectrum, a synthesized ring-wedge detector was used. For the experiments all objects to be Fourier transformed were illuminated in a way to achieve good quality in the black–white LCD image that is derived from the video image. As we were interested in learning and testing objects in different positions, they were mounted on an optical bench, their position was controlled by means of a mm scale.

In the SLM-unit, a rectangular aperture was placed in the read-out beam before the BSO/LC-SLM in order to avoid interaction of the coherent light with the limits of the LCD image. Additionally, the intensity of the focus spot could be reduced.

Some experiments with bright–dark edges as objects were carried out to describe the fundamental characteristics of the Fourier spectrum of light modulated in the BSO/LC-SLM. First, the spectrum of a stationary bright–dark edge was recorded for different driving voltages and polarizer orientations.It is presented as a grey-shade plot of the CCD matrix data. Furthermore disturbances in the spectrum of a moving edge were observed. Therefore the segment intensities (ten rings, 20 wedges) in the Fourier plane were recorded for five different velocities of the edge.

To examine the shift-invariance of the Fourier transform, the segment intensities were recorded for 30 equidistant (0·5 mm) positions of the test object.

Pattern recognition via numerical processing (section 4) was carried out for different applications. The reference objects were learned at a given position (30 mm), however the test objects had to be identified at different positions from 0 mm to 60 mm in steps of 2 mm. The development of the segment intensities square deviations are presented for following objects: a lensholder with/without screw and a bar 1 cm/2 cm/ . . . /6 cm tall. The number of rings and wedges was varied to get maximum discrimination.

To check the ability of the set-up for industrial inspection applications a printed circuit, a bottle and a glass with baby food were used as test objects.

(*c*) 10.4 *V*

(*d*) 13.3 *V*

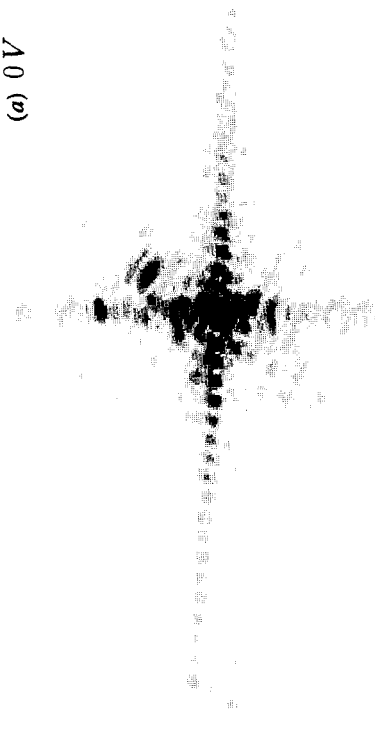

(*a*) 0 *V*

(*b*) 7.8 *V*

6. Results

6.1. *Edge spectrum*

Figure 2 shows the plot of a bright–dark edge spectrum at four different driving voltages. Both polarizers were orientated at 0° and thus edge enhancement is supported.

At zero voltage only the single slit diffraction pattern of the aperture is seen (figure 2 (*a*)). At 7 V the long asymmetric pattern of the edge that seems to be pointing into the dark (bright) side of the edge appears (see figure 2 (*b*) with 7·8 V). At higher voltages the edge pattern contains higher spatial frequencies indicating that the phase-modulated part of the edge has become smaller (see figure 2 (*c*) and (*d*) with 10·4 V respectively 13·3 V). This is due to the increased voltage gradient at the edge leading to an increased slope of the phase.

The small spots in the upper-right part of the spectrum result from a slightly curved stripe pattern that is superimposed to the images (figure 4). Spots and stripe patterns both rotate with the orientation of the BSO/LC-SLM. The stripe patterns may be a superposition of internal reflections in the device.

The asymmetric spectrum occurred even when no polarizers were in use. It was strongest when the LC director at the input side was parallel to the polarization, if perpendicular it almost vanished.

As we know from section 2.1 phase modulation occurs only in the first case, so the asymmetric edge spectrum can be explained with local phase variations at the edge.

This asymmetric edge spectrum is similar to those that one of us (H.-J. T.) [10, 11] observed at transparent–opaque edges of photographic film material.

6.2. *Velocity detection*

In figure 4 (*b*) is shown the coherent read-out image of a lensholder moved to the left. The edges of the object are enhanced. Those edges that are moving into the unilluminated part (outside the object) are small, those moving into the bright part are broadened considerably.

Corresponding to this, the results for a moving, almost upright bright–dark edge are shown in figure 3. In each of the four diagrams a certain segment that lies in the diffraction pattern of the edge is considered. One sees from top to bottom, following cases: Stationary edge, edge moving into dark with $10\,\mathrm{mm\,s^{-1}}$ respectively $30\,\mathrm{mm\,s^{-1}}$, edge moving into bright with $10\,\mathrm{mm\,s^{-1}}$ respectively $30\,\mathrm{mm\,s^{-1}}$. The edge was realized as a black cartridge before the white background. It was moved by pulling the mount by hand, so the velocities mentioned above are not very accurate.

When the bright–dark edge is shifted towards its dark side the intensity of the diffraction pattern is decreased.

This effect is due to changes of the intermediate zone when the edge is moving. We are led to the conclusion that the phase-modulated area (between 6 and 13 V effective voltage) is broadened and the decreased slope of the phase produces lower spatial frequencies. This broadening is due to the decay of BSO conductivity.

The results for edges moving into their dark side are not so easily understood. At low velocities ($10\,\mathrm{mm\,s^{-1}}$) the spectrum is brighter, at higher ones it is darker than that of the stationary edge (figure 3). Here, only theoretical studies of the dynamic electrical processes in the BSO/LC-SLM can give a satisfying explanation.

Amount and direction of an object's velocity can be obtained approximately from such a Fourier pattern (figure 3). This should apply also for two short light exposures of the BSO/LC-SLM.

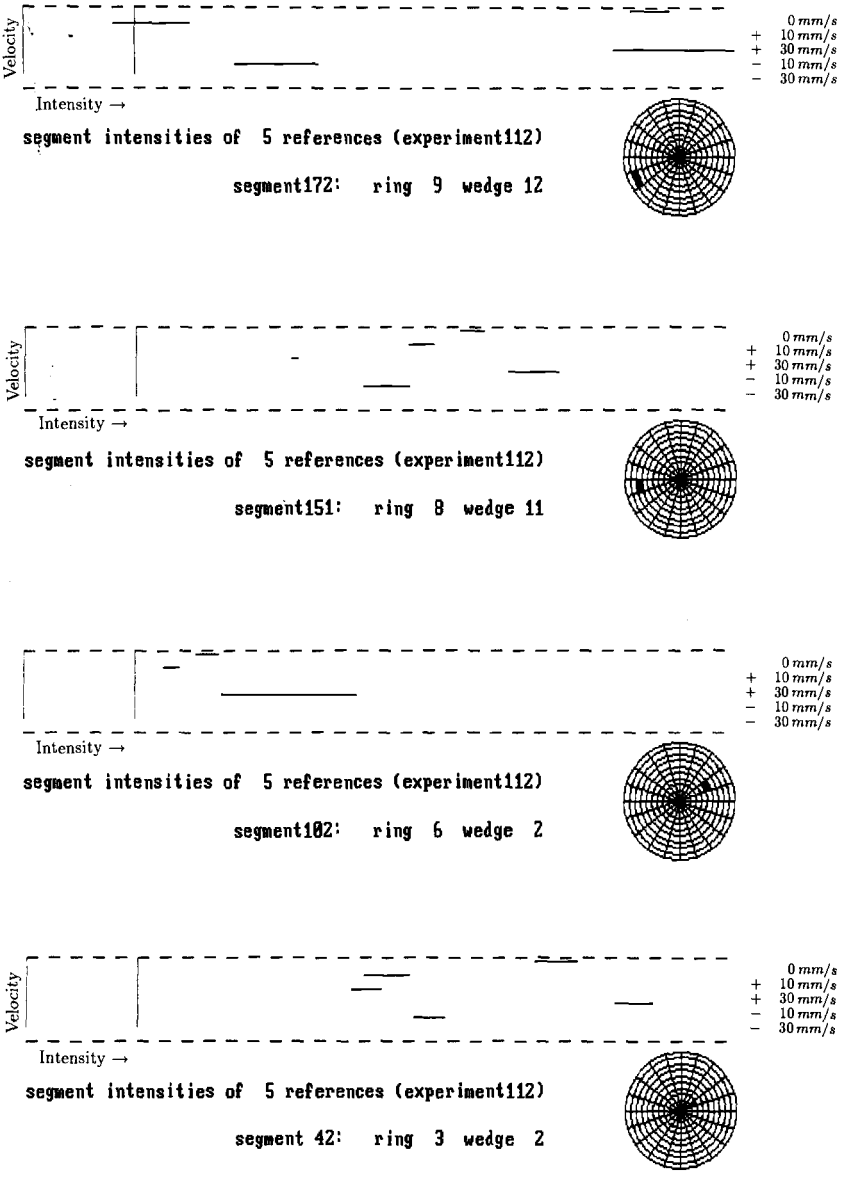

Figure 3. Detection of shift velocity of a bright–dark edge. The intensities of four ring-wedge segments are displayed. The horizontal axis of each diagram refers to the intensity (arbitrary unit), the vertical axis to the velocity of the edge (from top to bottom: stationary/slow and fast into the dark . . . /slow and fast into the bright side of the edge).

(*a*)

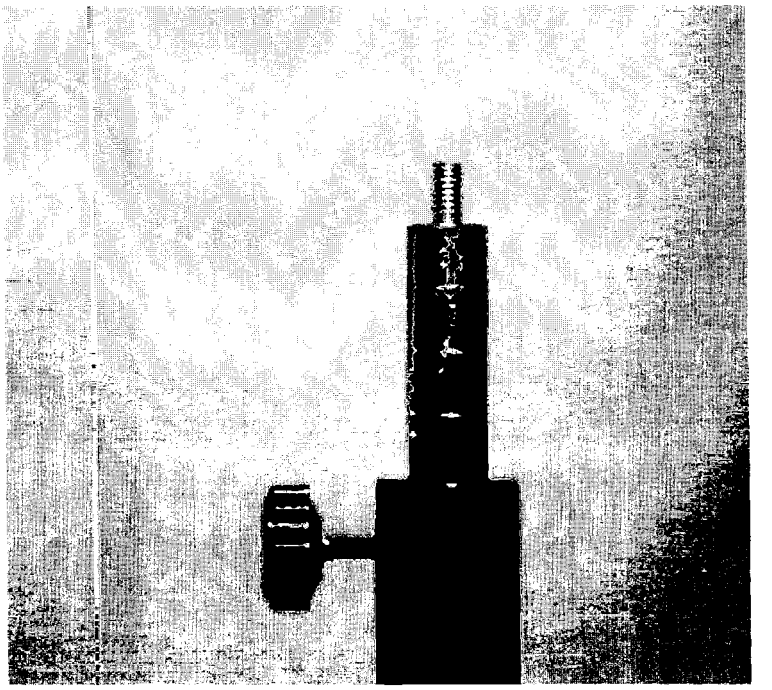

(*b*)

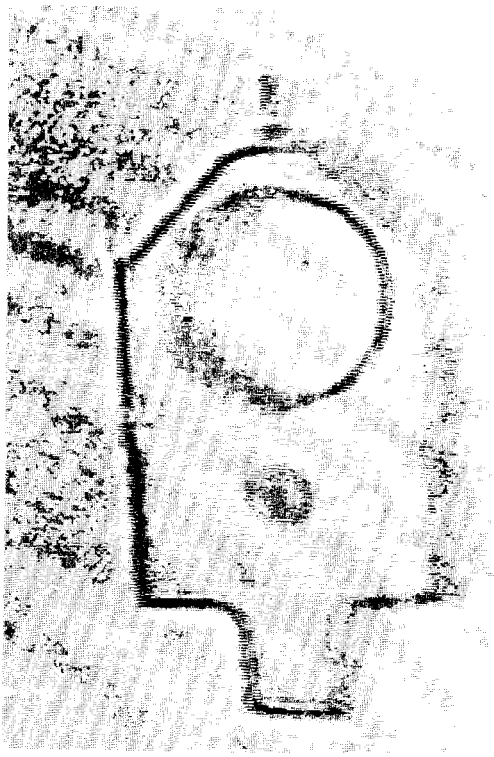

Figure 4. Images of test objects. (*a*) Bar, 4 cm tall and (*b*) lensholder with a screw on top, moving to the left: coherent image produced by the SLM unit.

6.3. *Position detection*

In our experiments the shift-invariance of the objects' Fourier power spectrum was violated. We saw two systems of grainy modulations moving against each other parallel to the shift. The Fourier plane segment intensities showed periodic modulations while shifting the object.

Figure 5 shows several segment intensities and their development when a lensholder was shifted 30 times 0·5 mm at each step. The driving voltage was 16·0 V.

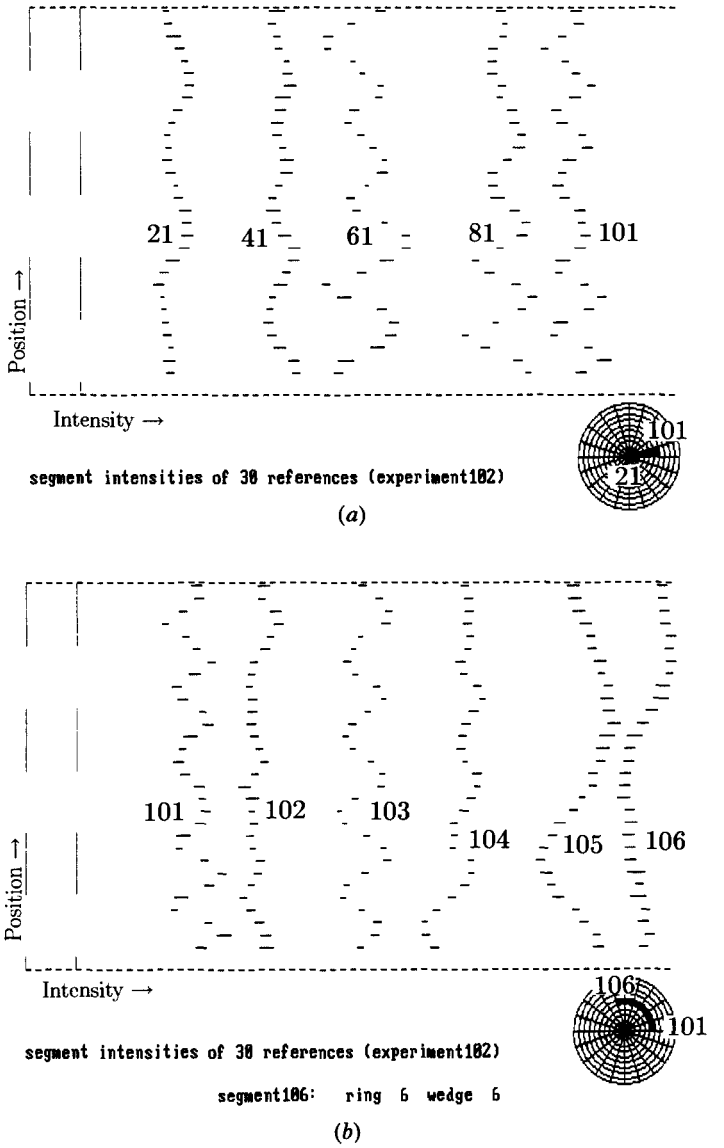

Figure 5. Intensity modulations of several segments in the Fourier plane while shifting an object. The Fourier plane is segmented with ten rings and 20 wedges. From left to right are displayed the intensities of following segments: (*a*) segments 21, 41, 61, 81, and 101. (*b*) segments 101, 102, 103, 104, 105, and 106.

The amplitude of the modulation had its maximum value at driving voltages above 18 V where the coherent light showed the sequence 'dark–bright–dark–very bright' at the transition from the dark to the illuminated side of the edge. Due to this shift-variance our pattern recognition technique was able to recognize the position of an object with an accuracy of 0·5 mm.

These intensity modulations were already reported in [12] for other experiments with spatial light modulators. A source of the modulations might be that the object is shifted, but the aperture is stationary. Further investigations to this phenomenon, especially numerical simulations, are in progress.

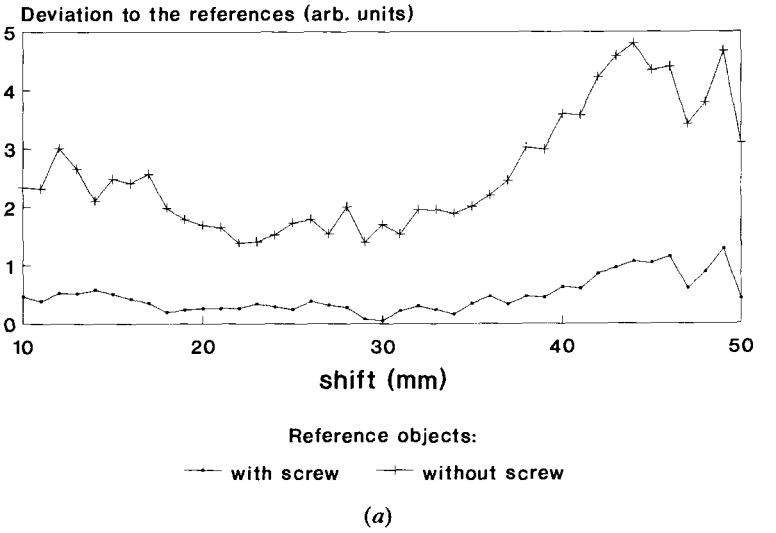

(*a*)

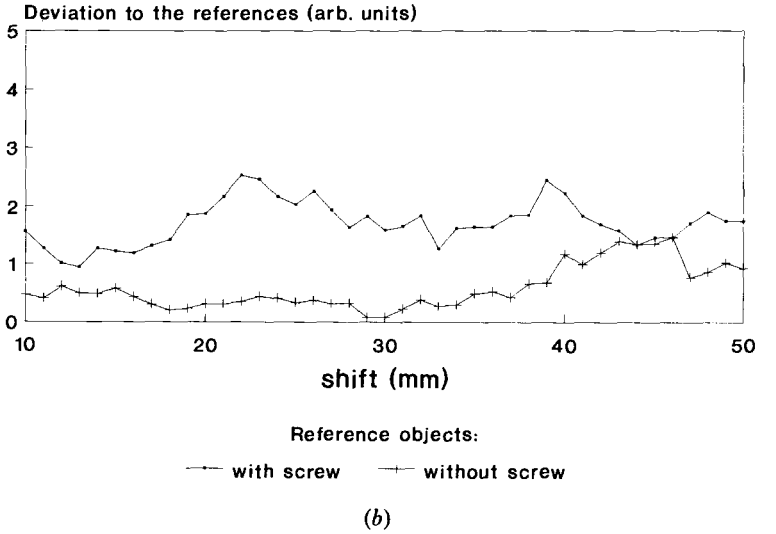

(*b*)

Figure 6. Lensholder learned with and without screw: deviations while testing on different positions. Test object was the lensholder (*a*) with screw, (*b*) without screw.

6.4. *Pattern recognition*

All experiments in this section were carried out with both polarizers at 0° and a driving voltage of 16 V to achieve an extended edge spectrum (see section 6.1.).

From the experiment follows that the concept of shift-invariant pattern recognition with optical Fourier transformation is severely affected by these modulations. Indeed, the deviation of the segment intensities with respect to the reference (learned at a given position) varied with the position of the object.

In the case of the lensholder (figure 6) the screw or its lack was easily detected at the learning position (30 mm), the ratio of the deviations (equation (1)) to the

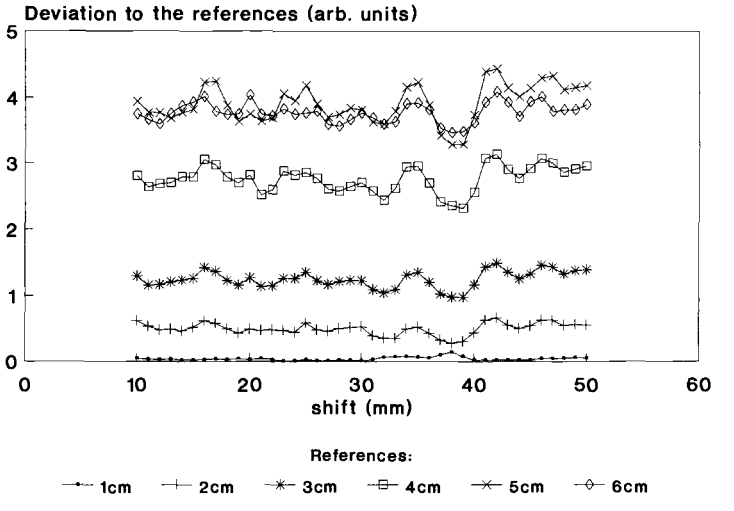

(*a*)

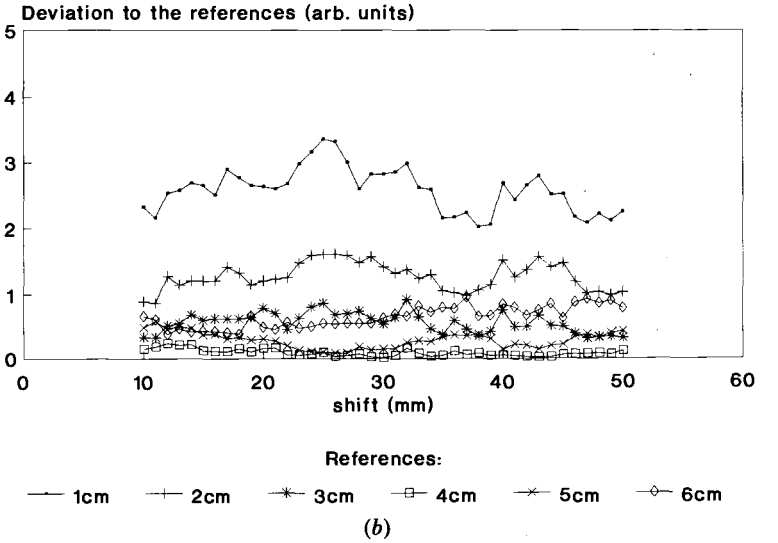

(*b*)

Figure 7. Bar learned with different lengths (1 cm/2 cm/ . . . /6 cm): deviations while testing on different positions. Test object was the bar with a length of (*a*) 1 cm, (*b*) 4 cm.

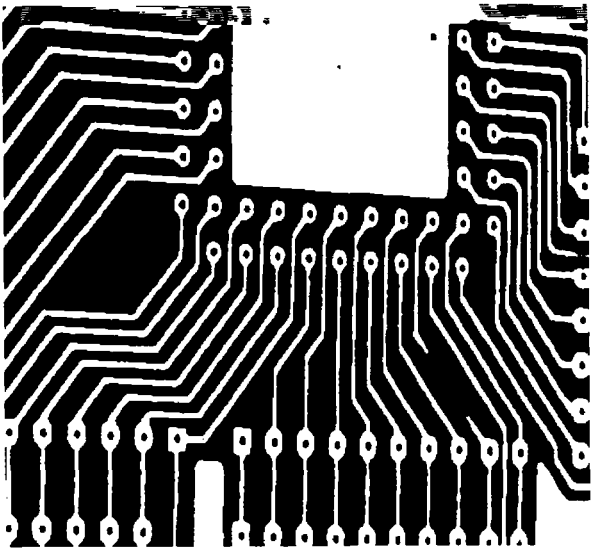

(*a*)

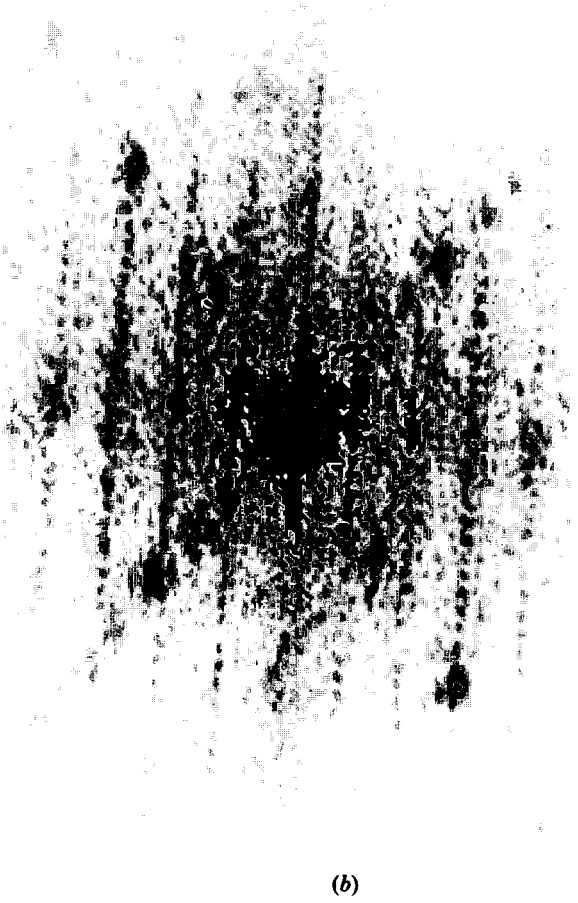

(*b*)

Figure 8. Printed circuit with defect (*a*) and the Fourier transform of its SLM image (*b*).

Table. Applications of the optical FT processor in pattern recognition.

Test object	Quadratic deviations to the references	
	Bottle with screw-top	Without screw-top
Bottle with screw-top	45...72	1348...1511
Without screw-top	1432...1620	7...22
	Correct baby food	Untight lid
Correct baby food	66...78	413...489
(different positions)	116...151	266...335
Untight lid		
(learning position)	601...637	3...7
(different positions)	602...693	52...71
	680...815	48...103
No object	1124...1150	1899...1971

references was about 1 : 200. On other positions the deviations were increased and their ratio was reduced to almost 1 : 2. On two positions the lens-holder without screw was not correctly recognized. The shifting range was twice the extension of the lensholder. Optimal discrimination was achieved with ten rings and 20 wedges for the segmentation of the Fourier plane. Discrimination quality could not be increased when a stop filter was placed in the first Fourier plane. The length of the bar was detected correctly over the whole shifting range (figure 7).

The position sensitivity of the deviations is certainly connected with the intensity modulations we reported in section 6.3.

Learning and testing at one given position allows for more difficult discrimination tasks. In an application the Fourier processor system recognized small defects in conductor lines of a printed circuit (figure 8) with a ratio of 1 : 10. Therefore a segmentation with three rings and 80 wedges was used.

Two examples of industrial application in pattern recognition are presented where binarization of the image is superior to a grey-shade representation. A segmentation with three rings and 80 wedges was used.

One task was to detect the screw-top on a bottle. Due to the binarization the screw-top (seen from above) appeared in the BSO/LC-SLM image as a filled circle, the bottle itself was invisible and thus one had not to deal with the position of the bottle's label. The bottle was learned with and without screw-top. The ratio of the quadratic deviations of right and wrong objects was around 1 : 30 when the shifting range of the bottle was several centimetres (see the table).

In the second example the tightness of glasses with baby food was controlled. Correctly, there is a vacuum inside the glass and the lid vaults to the inside; an untight lid is flat. The difference is visible when looking from laterally from above. The binarization increases the quality of pattern recognition because the lid's structure is pronounced and the inscription on the lid vanishes. When the glass was positioned with an accuracy of 0·5 cm (referred to the learning position) deviation ratios of at least 1 : 2 could be obtained (see the table).

7. Conclusions

We have presented a set-up for coherent-optical Fourier transformation of video images. The associated digital interpretation system allows quick learning and a pattern recognition frequency of 2 Hz. All components in use except the SLM unit

are not expensive and easily available, no ring-wedge CCD detector [8, 12] but a CCD matrix camera was used. The modulation characteristics of the optically addressed BSO/LC-SLM produced for bright–dark edges a largely extended and asymmetric Fourier spectrum. Thus an object's spectrum contains more information about its contours, compared to SLM with pixel structure. Rather similar objects could be discriminated even on different positions (e.g. the absence of a screw on a lensholder, see figure 4 and figure 6).

The SLM-unit might be replaced by an electrically addressed transmittive LCD. Another possibility would be to image the incoherently illuminated object directly into the BSO/LC-SLM to save the video camera and the LCD of the SLM-unit.

The relaxation time (75 ms) of the BSO/LC-SLM is slow compared to other optically addressed SLM, however it can be applied for dynamic data storage and detection of motions (section 6.2.).

Acknowledgments

We thank Bernd Schmidt for his contribution to the set-up. Furthermore we thank the Deutsche Forschungsgemeinschaft (DFG) for financial support. The experiments were carried out with an SLM-unit that Thomson-CSF provided for us.

References

[1] GÜNTER, P., and HUIGNARD, J. P., (editors), 1988, *Topics in Applied Physics*, **61**, (Berlin: Springer).
[2] HUIGNARD, J. P., HERRIAU, J. P., and VALENTIN, T., 1977, *Appl. Optics*, **16**, 11,
[3] TIZIANI, H. J., and KLENK, J., 1981, *Appl. Optics*, **20**, 1467.
[4] LOISEAUX, B., ILLIAQUER, G., and HUIGNARD, J. P., 1985, *Opt. Engng.*, **24**, 144–9.
[5] Final report *Spatial light modulators for 2D optical processor* of the ESPRIT-project 1035 *2D coherent optical dynamic processor*, Thomson-CSF Laboratoire Central de Recherches, Labo. 085/BL.
[6] EFRON, U., 1989, *Proc. SPIE*, **960**, 180.
[7] CASASENT, D., and RICHARDS, J., 1988, *Opt. Engng*, **27**, 285.
[8] CLARK, D., and CASASENT, D., 1988, *Opt. Engng.*, **27**, 365.
[9] CASASENT, D., and RICHARDS, J., 1988, *Appl. Optics*, **27**, 4653.
[10] TIZIANI, H. J., BEYELER, B. H., and WITZ, W., 1970, *Optics Technol.*, **2**, 75.
[11] TIZIANI, H. J., and WITZ, W., 1971, *Optik*, **32**, 484.
[12] KASDEN, N. H., 1979, *Opt. Engng.*, **18**, 496.